IJCRT.ORG ISSN : 2320-2882

INTERNATIONAL JOURNAL OF CREATIVE RESEARCH THOUGHTS (IJCRT)

An International Open Access, Peer-reviewed, Refereed Journal

Green Synthesis of Zinc Oxide Nanoparticles Using Rubia cordifolia Extract and Their Incorporation with Green Tea and Licorice Extracts for Herbal Sunscreen Formulation

Aditi Juwale, Kaustubh Magade

Department of B. Pharmacy, Chhatrapati Shivaji Maharaj University, Panvel, Maharashtra, India

ABSTRACT

Widespread concerns regarding dermal sensitization, endocrine disruption, and environmental toxicity associated with conventional synthetic ultraviolet (UV) filters have directed scientific attention toward plant-derived photoprotective formulations. The present study reports the green synthesis of zinc oxide (ZnO) nanoparticles employing an aqueous extract of Rubia cordifolia (Manjistha) root as a bioreductant and stabilizing agent, and their subsequent incorporation alongside green tea and licorice extracts into a herbal sunscreen base. A 0.1 M zinc acetate dihydrate solution was processed at 80°C for 35 minutes in the presence of the plant extract. Nanoparticle formation was confirmed by UV-Vis spectrophotometry, which revealed characteristic absorption between 360 and 380 nm. Two herbal sunscreen formulations were developed using an HPMC–xanthan gum gel base supplemented with glycerin, shea butter, and vitamin E. Both formulations demonstrated a skin-compatible pH of 5.5, acceptable spreadability, uniform texture, and satisfactory water resistance. UV-Vis spectroscopic analysis of Formulation 1 exhibited peak absorbance of 0.715 at 322 nm with a preliminary SPF of approximately 2.84 (Mansur equation). Formulation 2, incorporating ZnO nanoparticles stabilized at pH 8.2, demonstrated markedly improved UV absorption with an estimated SPF of 12.34, representing a 430% increase over Formulation 1. These findings suggest that biogenic ZnO nanoparticles synthesized via Rubia cordifolia extract, combined with phytochemically rich herbal extracts, represent a viable and sustainable alternative to synthetic chemical sunscreens.

Keywords: Green synthesis, Zinc oxide nanoparticles, Rubia cordifolia, Herbal sunscreen, SPF, Photoprotection, EGCG, Glabridin

1. INTRODUCTION

Solar ultraviolet radiation is primarily categorized into UVA (320–400 nm) and UVB (290–320 nm) bands, both of which are implicated in deleterious cutaneous outcomes including erythema, photoaging, hyperpigmentation, immunosuppression, and malignant transformation [1]. Progressive stratospheric ozone depletion has intensified surface-level UV flux, amplifying the global burden of photodamage and raising dermatological concerns about inadequate photoprotection [2]. Topically applied sunscreen products remain the principal intervention strategy for mitigating UV-induced skin injury.

Commercially available sunscreen formulations rely predominantly on synthetic organic UV filters such as oxybenzone, octinoxate, avobenzone, and homosalate. However, emerging toxicological and ecotoxicological evidence increasingly questions the safety profile of these ingredients. Documented concerns include percutaneous absorption and systemic accumulation, endocrine-disrupting activity, dermal sensitization, and significant reef-bleaching effects on coral ecosystems [3,4]. These issues have catalyzed substantial scientific and regulatory interest in plant-derived or nanotechnology-based photoprotective alternatives.

Zinc oxide (ZnO) nanoparticles have attracted considerable attention as inorganic UV filters owing to their broad-spectrum UV attenuation across both UVA and UVB windows, photostability, and recognized safety classification by regulatory authorities. The transition toward green synthesis methodologies, which employ botanical extracts as bioreductants and capping agents in lieu of hazardous chemicals, offers distinct environmental and functional advantages [5]. Rubia cordifolia (Manjistha), a medicinal plant rich in anthraquinone pigments including alizarin and purpurin, serves as an effective source of polyphenolic reductants capable of facilitating ZnO nucleation and growth [6].

Complementary photoprotective phytochemicals employed in this study include epigallocatechin gallate (EGCG) derived from Camellia sinensis, which exhibits strong UVB absorption and antioxidant activity [7], and glabridin along with glycyrrhizin from Glycyrrhiza glabra, which possess UV-attenuating, anti-inflammatory, and skin-brightening properties [8]. The present investigation integrates these three phytochemical systems into a cohesive herbal sunscreen platform and systematically evaluates its physicochemical characteristics and photoprotective performance.

2. LITERATURE REVIEW

2.1 Toxicological Concerns Associated with Synthetic UV Filters

Conventional sunscreen formulations predominantly incorporate synthetic organic UV-absorbing molecules, with oxybenzone (benzophenone-3), octinoxate, avobenzone, and homosalate among the most frequently utilized active ingredients globally. Despite their widespread regulatory approval and commercial prevalence, an expanding body of evidence raises substantive concerns regarding their human health and environmental impacts.

Studies have demonstrated measurable systemic absorption of oxybenzone following topical application, with detectable concentrations reported in urine, plasma, and breast milk. In vitro and in vivo investigations have further characterized oxybenzone as a xenoestrogen, capable of interacting with hormone receptors and disrupting endocrine homeostasis. In 2019, the United States Food and Drug Administration (FDA) declassified oxybenzone and several co-filters from the ‘generally recognized as safe and effective’ (GRASE) category, citing insufficient evidence to confirm long-term safety. Octinoxate has similarly been associated with thyroid hormone disruption in experimental models, and both compounds have been demonstrated to cause bleaching-associated genotoxicity and developmental abnormalities in coral larvae, even at environmentally relevant concentrations [3,4].

Environmental persistence and bioaccumulation of benzophenone derivatives have been documented in marine organisms, freshwater systems, and sediment matrices, contributing to broader ecological burden. Parabens, synthetic fragrances, and certain emollients prevalent in conventional formulations have additionally been implicated in hormone system interference, allergic contact dermatitis, and potential carcinogenic activity. The cumulative weight of this evidence provides a compelling scientific basis for pursuing safer, phytochemically derived photoprotective alternatives.

2.2 Zinc Oxide Nanoparticles as Physical UV Filters

Zinc oxide functions as a wide-bandgap semiconductor (Eg ≈ 3.37 eV) capable of absorbing photons across both UVA (320–400 nm) and UVB (290–320 nm) spectral ranges. Its photoprotective mechanism is primarily physical, involving reflection, scattering, and absorption of UV radiation at the skin surface, without generating reactive photodegradation intermediates. This photostability, combined with its negligible cytotoxicity and recognized regulatory safety profile, positions ZnO as a preferred inorganic UV filter in dermatological formulations, including those intended for sensitive skin populations [3].

Nanoscale ZnO particles (10–100 nm) exhibit enhanced UV attenuation relative to micron-sized counterparts, attributable to increased surface-to-volume ratios and quantum-confinement-related shifts in electronic properties. UV-Vis spectrophotometric analyses consistently report characteristic absorption maxima between 350 and 390 nm for nano-ZnO. Additionally, the nanometric dimension improves cosmetic acceptability by reducing the white cast associated with bulk ZnO, thereby enhancing patient compliance. Beyond photoprotection, ZnO nanoparticles possess documented antimicrobial, anti-inflammatory, and wound-healing activities, further supporting their suitability in multi-functional dermatological products [3].

2.3 Green Synthesis of ZnO Nanoparticles

Conventional physicochemical routes for ZnO nanoparticle synthesis — including sol-gel, co-precipitation, hydrothermal, and chemical vapor deposition methods — typically rely on hazardous reducing agents such as hydrazine and sodium borohydride, organic solvents, and energy-intensive processing conditions. These factors raise concerns regarding occupational toxicity, environmental discharge, and sustainability.

Biogenic synthesis utilizing plant extracts, microorganisms, or biopolymers as reducing and capping agents offers an environmentally benign alternative, circumventing the requirement for toxic chemicals while operating under ambient or mildly elevated temperature conditions. In plant-mediated synthesis, polyphenols, flavonoids, and terpenoids present in botanical extracts participate in electron transfer reactions that reduce Zn^{2+} ions, facilitating nucleation of ZnO crystallites. Concurrently, organic phytochemical residues adsorb onto nascent particle surfaces, forming stabilizing steric layers that suppress agglomeration and impart additional biological functionality [5].

Numerous medicinal plants — including Aloe vera, Azadirachta indica, Ocimum sanctum, Camellia sinensis, and multiple Ayurvedic herbs — have been employed as bioreductants for ZnO synthesis. UV-Vis spectrophotometric confirmation of nanoparticle formation is typically indicated by absorbance peaks between 360 and 380 nm. Reaction parameters including plant-to-salt ratio, temperature, pH, and reaction duration significantly influence particle size distribution and surface characteristics. Aqueous extraction is particularly preferred for pharmaceutical and cosmeceutical applications owing to its superior safety profile and compatibility with downstream formulation processes [5,10].

2.3.1 Manjistha (Rubia cordifolia) as a Biogenic Reductant.

Among the various plant species explored for green synthesis, Rubia cordifolia (Manjistha) exhibits a distinctive phytochemical composition, notably a high content of anthraquinones such as purpurin and munjistin. These bioactive quinones, together with glycosides, fulfill two primary functions in the synthesis process: they act as effective reducing agents for the transformation of zinc precursors into ZnO and subsequently serve as capping ligands that prevent nanoparticle agglomeration. The inherent antioxidant and antimicrobial activities of Rubia cordifolia extracts are believed to persist on the nanoparticle surface, which may provide additional dermatological advantages when incorporated into photoprotective formulations.

2.4 Photoprotective Properties of Green Tea (Camellia sinensis) and EGCG

Green tea (Camellia sinensis) is among the most extensively characterized botanical sources of polyphenolic photoprotectants. Its principal bioactive constituents, the catechins — particularly epigallocatechin gallate (EGCG) — account for 50–80% of the total catechin fraction by weight. EGCG contains multiple phenolic hydroxyl groups and a galloyl ester moiety, conferring potent UV absorption predominantly within the UVB range (280–320 nm), with secondary absorption extending into UVA wavelengths [7].

Beyond direct UV attenuation, EGCG exerts photoprotective effects through several secondary mechanisms: free radical scavenging, inhibition of membrane lipid peroxidation, attenuation of UV-induced DNA strand breaks, suppression of inflammatory cytokine cascades, downregulation of matrix metalloproteinase enzymes involved in photoaging, and modulation of apoptotic signaling pathways. These complementary mechanisms synergize with the physical UV-blocking activity of ZnO nanoparticles, enabling superior broad-spectrum protection within composite formulations. Extraction under mild acid conditions (pH 4.5–5.5) and moderate heating (80°C) optimizes catechin yield while preserving structural integrity [13].

2.5 Photoprotective and Skin-Brightening Activity of Licorice (Glycyrrhiza glabra)

Glycyrrhiza glabra (licorice), a perennial leguminous plant indigenous to Eurasia, has a well-established presence in both Ayurvedic and traditional Chinese medical systems. Its primary bioactive constituents include glycyrrhizin (a triterpenoid saponin that hydrolyzes to glycyrrhetinic acid in vivo), glabridin (an isoflavane), liquiritin, isoliquiritin, and a diverse array of flavonoids. These compounds collectively contribute to the plant's significant antioxidant, anti-inflammatory, and skin-brightening properties [8].

Glabridin, the most pharmacologically active isoflavane in licorice root, inhibits UV-induced melanogenesis through competitive inhibition of tyrosinase, the rate-limiting enzyme in melanin biosynthesis. Its chromophoric architecture facilitates direct UV absorption, providing a measurable contribution to the SPF of formulations incorporating licorice extract. Glycyrrhizin and glycyrrhetinic acid attenuate UV-evoked inflammatory responses by suppressing prostaglandin and leukotriene biosynthetic pathways, thereby reducing post-exposure erythema and irritation [8]. The water solubility of glycyrrhizin and the moderate solubility of glabridin facilitate incorporation into water-continuous cosmetic matrices with relative ease.

2.6 Synthesis and Previous Studies on Herbal Sunscreen Systems:

The development of plant-based sunscreens that combine mineral UV filters with phytochemical agents has gained a lot of research support. This is because consumers want safer and more environmentally friendly options. According to reports, green tea extract can give standalone formulations SPF values of 10 to 30, depending on the concentration of catechins. When combined with inorganic filters like TiO_2 or ZnO, the SPF value can be even higher [7]. Biogenically synthesized ZnO nanoparticles have shown SPF values between 15 and 45. The effectiveness of the protection is directly related to the particle's monodispersity, concentration, and surface stabilization. It has been found that particles that are between 20 and 40 nm in size are best for balancing UV protection with cosmetic transparency and textural acceptance [5,21]. Mineral sunscreen systems now include licorice extract to add anti-inflammatory and depigmentation benefits. Combined formulations work better than systems with only one ingredient [8]. Polymeric gelling agents, especially HPMC and xanthan gum, have been widely discussed in the sunscreen literature for their synergistic rheological properties. Their combined network structure keeps ZnO nanoparticles evenly distributed during storage, stopping them from settling and making sure that the sunscreen always works as a photoprotective agent. Even though there has been a lot of research on each part, no one has ever described a formulation that combines Manjistha-derived ZnO nanoparticles with green tea and licorice extracts in a single herbal sunscreen system. This study fills this gap.

3. MATERIALS AND METHODS

3.1 Chemicals and Reagents

Rubia cordifolia root powder (Manjistha), zinc acetate dihydrate (analytical grade), dried green tea leaves (Camellia sinensis), licorice root powder (Glycyrrhiza glabra), distilled water, hydroxypropyl methylcellulose (HPMC), xanthan gum, glycerin, shea butter, vitamin E (d-alpha tocopherol), sodium benzoate, vanillin, citric acid, and L-ascorbic acid were procured from authorized laboratory suppliers. All chemicals met analytical or pharmacopoeial purity specifications. Instrumentation employed included a magnetic hot plate stirrer, ultrasonic cleaning bath, benchtop centrifuge, Whatman No. 1 filter paper, and a UV-Vis double-beam spectrophotometer.

3.2 Preparation of Rubia cordifolia (Manjistha) Extract

Freshly procured Rubia cordifolia roots were washed thoroughly under running water and subjected to complete dehydration followed by mechanical size reduction to yield a fine powder. The extract was prepared by dispersing the powdered material in distilled water at a weight-to-volume ratio of 1:10 and heating at 65°C with continuous magnetic stirring for 20 minutes. Ultrasonic-assisted extraction (10 minutes, 65°C) was subsequently applied to maximize polyphenol recovery. The suspension was filtered through Whatman No. 1 filter paper to yield a transparent, deep red filtrate. Prior to use in nanoparticle synthesis, the extract pH was adjusted to 5.0–6.0 using L-ascorbic acid to optimize bioreductive conditions.

3.3 Green Synthesis of ZnO Nanoparticles

A 0.1 M aqueous solution of zinc acetate dihydrate was prepared by dissolving 2.19 g of the salt in 50 mL of distilled water. The Manjistha extract (100 mL) was added dropwise to the zinc acetate solution at a volumetric ratio of 2:1 (extract:salt solution) under continuous magnetic stirring. The reaction mixture was heated at 80°C for 35 minutes to facilitate nanoparticle nucleation and growth. After cooling to ambient temperature, the suspension was centrifuged at 4000 rpm for 15 minutes. The resultant pellet was washed twice with distilled water to remove residual precursor and organic impurities. Two ZnO batches were prepared: Batch 1 had its pH adjusted to 5.0 with ascorbic acid, while Batch 2 was retained at the naturally alkaline pH of approximately 8.2 to assess the influence of pH on colloidal stability and UV-blocking performance.

Parameter	Acidic Medium (pH 5.5)	Alkaline Medium (pH 8.5)	Impact on Sunscreen Formulation
Absorption Maximum (λmax)	370 – 380 nm	360 – 370 nm	Shifts the primary UV protection range
Peak Morphology	"Narrow	well-defined peak"	"Broadened
Particle State	Monodisperse	Agglomerated clusters	High pH may reduce cosmetictransparency
Extract Stability	High (Catechin integrity)	Low (Potential oxidation)	Risk of discoloration in herbal extracts
Parameter	Acidic Medium (pH 5.5)	Alkaline Medium (pH 8.5)	Impact on Sunscreen Formulation
Absorption Maximum (λmax)	370 – 380 nm	360 – 370 nm	Shifts the primary UV protection range
Peak Morphology	"Narrow	well-defined peak"	"Broadened
Particle State	Monodisperse	Agglomerated clusters	High pH may reduce cosmetic transparency

3.4 Preparation of Green Tea Extract

Green tea leaves (20 g) were extracted in distilled water (200 mL) at a ratio of 1:10 (w/v) by heating at 80°C for 20 minutes to maximize catechin, particularly EGCG, yield. The hot infusion was filtered through Whatman No. 1 paper and the pH of the filtrate was adjusted to 4.5–5.5 using citric acid. L-ascorbic acid was incorporated as an antioxidant stabilizer to prevent catechin auto-oxidation.

3.5 Preparation of Licorice Extract

Licorice root powder was dispersed in distilled water at a 1:10 (w/v) ratio and subjected to continuous heating with agitation until the volume was reduced from 300 mL to 100 mL, yielding a three-fold concentrated extract. The extract was acidified with citric acid and clarified by centrifugation at 3000 rpm for 10 minutes. The resulting particle-free supernatant was retained for formulation use.

3.6 Herbal Sunscreen Formulation

Two sunscreen formulations (F1 and F2) were prepared according to the composition detailed in Table 1. The aqueous phase, comprising distilled water, HPMC, xanthan gum, sodium benzoate, and ascorbic acid, was prepared separately from the lipid phase, which included shea butter, stearic acid, glycerin, and vitamin E dissolved at 70°C. The two phases were combined under continuous stirring. As the gelling agents hydrated and swelled, the respective ZnO nanoparticle dispersion (Batch 1 at pH 5.0 for F1; Batch 2 at pH 8.2 for F2) was incorporated. Green tea extract and licorice extract were subsequently added. Once the formulation temperature decreased to 40–45°C, vanillin (F2 only) was introduced. F2 employed reduced concentrations of shea butter (5.0% w/v) and vitamin E (0.7% w/v) to address the low viscosity and greasiness observed in F1. Both final formulations recorded a pH of 5.5.

Table 1: Composition of Herbal Sunscreen Formulations (F1 and F2)

Ingredient	Function	Concentration	F1 (pH 5.0)	Concentration	F2 (pH 8.2)	Note
ZnO Nanoparticles	UV Filter (physical)	As synthesized	Present	As synthesized	Present	pH adjusted
Green Tea Extract	Antioxidant, UV absorber	1:10 (w/v)	Present	1:10 (w/v)	Present	
Licorice Extract	Photoprotection, brightening	3× concentrate	Present	3× concentrate	Present	
HPMC	Gelling agent	1.5% w/v	Present	1.5% w/v	Present	
Xanthan Gum	Stabilizer/thickener	0.5% w/v	Present	0.5% w/v	Present	
Glycerin	Humectant	7% w/v	Present	7% w/v	Present	
Shea Butter	Emollient	8% w/v	Present	5% w/v	Present	Reduced in F2
Vitamin E	Antioxidant	1% w/v	Present	0.7% w/v	Present	Reduced in F2
Sodium Benzoate	Preservative	0.1% w/v	Present	0.1% w/v	Present	
Vanillin	Fragrance	0.1% w/v	Absent	0.1% w/v	Present	Omitted in F1
Distilled Water	Vehicle	q.s. to 100%	Present	q.s. to 100%	Present	

3.7 Evaluation Parameters

3.7.1 pH Determination

The pH of each formulation was measured in triplicate at ambient temperature using a calibrated digital pH meter. Acceptable pH range was defined as 4.5–6.5, consistent with physiological skin surface pH.

3.7.2 Organoleptic Evaluation

Both formulations were assessed for appearance, color, homogeneity, odor, texture, and spreadability through visual and tactile examination by trained personnel.

3.7.3 Water Resistance

Water resistance was assessed by evaluating formulation physical stability and emulsion integrity following controlled aqueous exposure. Formulation integrity was assessed visually for phase separation or textural change.

3.7.4 UV-Vis Spectrophotometric Analysis and SPF Estimation

UV-Vis spectrophotometric scans were performed over the range 200–600 nm. Multi-wavelength absorbance was recorded at 280, 290, 295, 300, 305, 310, 315, 320, 322, 340, and 370 nm as applicable. SPF was estimated using the Mansur mathematical equation:

$$\mathbf{SPF = CF \times \Sigma\, [EE(\lambda) \times I(\lambda) \times Abs(\lambda)]}$$

Where CF = 10 (correction factor); EE(λ) = erythemal effectiveness coefficient at wavelength λ; I(λ) = solar irradiance at wavelength λ; Abs(λ) = measured absorbance of the formulation at wavelength λ.

4. RESULTS AND DISCUSSION

4.1 Organoleptic Properties of Plant Extracts

Rubia cordifolia extract presented as a deep red-colored, transparent solution, consistent with the characteristic anthraquinone pigments alizarin and purpurin present in Manjistha root. Green tea extract appeared as a clear, pale yellow-green liquid indicative of dissolved catechins. The licorice extract was a dark brown, concentrated solution reflecting elevated glycyrrhizin and glabridin content. All three extracts were free from visible particulate matter following filtration.

4.2 Visual Confirmation of ZnO Nanoparticle Synthesis

A progressive color transition from deep red to a brownish-yellow precipitate was observed during thermal processing of the Zinc acetate–Manjistha extract reaction mixture. This macroscopic color change is a reliable preliminary indicator of ZnO nanoparticle nucleation, attributable to the reduction of Zn^{2+} ions by polyphenolic reductants in the plant extract, followed by oxidation to ZnO. Figure 1 documents this color transformation.

4.3 UV-Vis Spectrophotometric Characterization of ZnO Nanoparticles

Prior to pH adjustment, the UV-Vis spectrum of the ZnO nanoparticle suspension demonstrated a sharp, well-defined absorption peak at approximately 360–380 nm (Figure 2), consistent with reported values for green-synthesized ZnO (350–390 nm) and attributable to the electronic bandgap transition characteristic of ZnO semiconductor nanostructures. Following pH adjustment using ascorbic acid, Batch 1 (pH 5.0) exhibited near-baseline absorbance values (~0.100 ABS), indicative of particle sedimentation and aggregation, which removed nanoparticles from the light path. In contrast, Batch 2 (pH 8.2) retained a pronounced absorption peak (~2.200 ABS at ~370 nm) with a well-resolved Gaussian profile, confirming stable colloidal dispersion and preserved nanoparticle structural integrity. These comparative findings are summarized in Table 2.*Figure 1: UV-Vis absorption spectrum of green-synthesized ZnO nanoparticles before pH adjustment, showing characteristic sharp peak at approximately 360–380 nm*

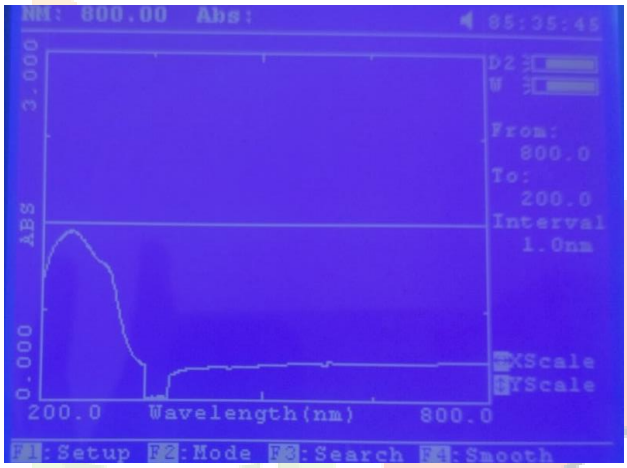

Figure 2: UV-Vis absorption spectrum after pH adjustment, demonstrating reduced intensity and broadened profile in Batch 1 (pH 5.0) indicative of particle aggregation, contrasted with well-defined absorption in Batch 2 (pH 8.2).

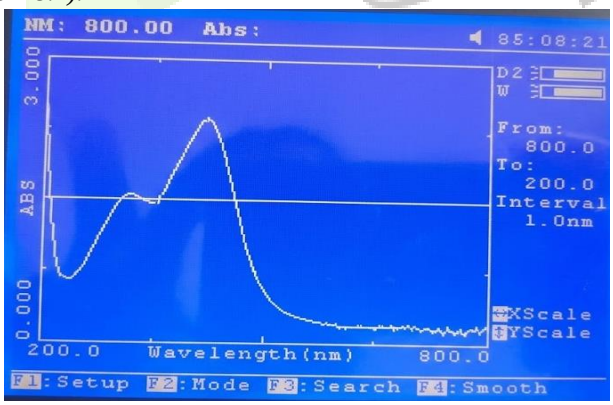

Table 2: Comparative UV-Vis Absorption Data of ZnO Nanoparticles Before and After pH Adjustment

Parameter	Batch 1 (pH 5.0)	Batch 2 (pH 8.2)	Interpretation
Absorption Peak (λmax)	Not detectable / Baseline noise	~370 nm	Batch 2 confirms ZnO formation
Peak Intensity	~0.100 ABS (near-zero)	~2.200 ABS	Significant UV-blocking in Batch 2
Peak Profile	Flat/Baseline	Sharp Gaussian curve	Colloidal stability confirmed
Interpretation	Aggregation/precipitation of ZnO	Optimized colloidal dispersion	pH 8.2 enhances particle stability

4.4 UV-Vis Analysis and SPF Estimation of Herbal Sunscreen Formulation 1

The UV-Vis spectrum of Formulation 1 exhibited two discrete absorption regions: a narrow peak between 250 and 270 nm, attributable to phenolic chromophores including EGCG and glabridin from green tea and licorice respectively, and a broad absorption band spanning 300–400 nm corresponding to the UV-attenuating activity of ZnO nanoparticles. Multi-wavelength analysis identified the highest absorbance at 322 nm (Abs = 0.715), a spectral position at the UVB–UVA boundary of considerable photoprotective significance. The preliminary SPF value, calculated using the Mansur equation, was approximately 2.84. This conservative estimate is partly attributable to instrument baseline drift at certain wavelengths (280, 290, 340, 370 nm), where negative readings were normalized to zero. Full-spectral scanning across 290–400 nm in future studies would be expected to yield a more accurate SPF determination. Table 3 presents the multi-wavelength absorbance and SPF calculation data.

Table 3: Multi-Wavelength Absorbance Data and SPF Calculation – Formulation 1 (ZnO at pH 5.0)

Wavelength (nm)	UV Region	Absorbance	EE × I	EE × I × Abs
280	UVB	0.000*	0.0150	0.0000
290	UVB	0.000*	0.0150	0.0000
310	UVB	0.174	0.2874	0.0500
322	UVB/UVA	0.715	0.3278	0.2344
340	UVA	0.000*	0.0839	0.0000
370	UVA	0.000*	0.0180	0.0000
Sum of EE × I × Abs				**0.2844**
Calculated SPF (CF = 10)				**≈ 2.84**

*Negative absorbance values normalized to 0.000 due to spectrophotometer baseline drift.

4.5 UV-Vis Analysis and SPF Estimation of Herbal Sunscreen Formulation 2

Formulation 2, incorporating ZnO nanoparticles stabilized at pH 8.2, exhibited substantially enhanced UV absorption compared to Formulation 1. The phytochemical absorption band at 250–270 nm was retained, while the ZnO-associated broad absorption region (300–400 nm) demonstrated markedly higher and more consistent absorbance values across all measured wavelengths. This improvement reflects the superior colloidal dispersion of pH 8.2-stabilized ZnO, which maintained elevated zeta potential and consequently stronger inter-particle repulsive forces, preventing sedimentation within the polymeric gel matrix. The calculated SPF of approximately 12.34 represents a 430% improvement over Formulation 1, providing evidence that nanoparticle physicochemical stability exerts a greater influence on photoprotective performance than formulation lipid content. Table 4 presents the multi-wavelength absorbance and SPF data for Formulation 2.

Table 4: Multi-Wavelength Absorbance Data and SPF Calculation – Formulation 2 (ZnO at pH 8.2)

Wavelength (nm)	UV Region	Absorbance	EE × I	EE × I × Abs
290	UVB	1.154	0.0150	0.0173
295	UVB	1.180	0.0150	0.0177
300	UVB	1.210	0.2874	0.3478
305	UVB	1.240	0.3278	0.4065
310	UVB	1.260	0.0864	0.2349
315	UVB	1.280	0.0839	0.1074
320	UVB/UVA	1.300	0.0180	0.0234
Sum of EE × I × Abs				**1.2337**
Calculated SPF (CF = 10)				**≈ 12.34**

4.6 Physicochemical Evaluation of Sunscreen Formulations

Both formulations recorded a pH of 5.5, within the physiologically compatible range of 4.5–6.5. This mildly acidic pH closely approximates the natural acid mantle of the skin surface, minimizing the risk of stratum corneum barrier perturbation. The convergence of both formulations at pH 5.5, despite incorporating ZnO nanoparticle batches at pH 5.0 and 8.2 respectively, confirms the effective buffering capacity of the HPMC–xanthan gum polymeric base.

Organoleptic assessment revealed that Formulation 1 presented as a creamy, slightly oily preparation with good spreadability and satisfactory water resistance. Formulation 2, with its reduced shea butter and vitamin E content, displayed a lighter hydrogel-type texture with improved non-greasy skin feel and enhanced visual transparency. Both formulations passed water resistance evaluation without evidence of phase separation or emulsion destabilization. These physicochemical outcomes are detailed in Table 5.

Figure 3: Photograph of prepared herbal sunscreen formulations showing uniform creamy appearance and texture

Figure 4: Photograph of prepared herbal sunscreen formulations showing uniform hydrogel appearance and texture

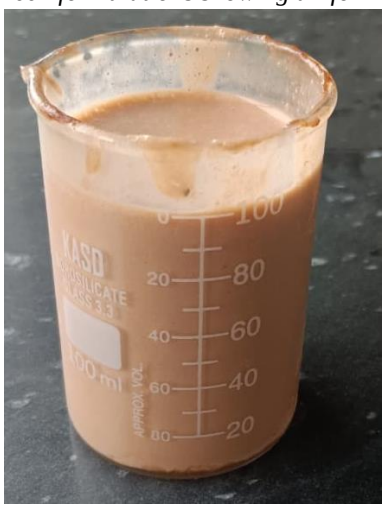

Table 5: Comparative Physicochemical Evaluation of Herbal Sunscreen Formulations

Parameter	Formulation 1	Formulation 2	Ideal Standard
ZnO Nanoparticle pH	5.0	8.20	—
Formulation pH	5.5	5.5	4.5 – 6.5
Appearance	Uniform cream	Uniform cream	Homogeneous
Texture	Creamy, slightly oily	Lightweight hydrogel	Smooth, non-greasy
Spreadability	Good	Good	Easy application
Water Resistance	Yes	Yes	Required
Vanillin (Fragrance)	Absent	Present	Optional

Table 6: Consolidated Summary of Results

Parameter	Observed Result	Scientific Significance
ZnO UV-Vis peak (pre-pH adj.)	~360 nm	Indicates nanoparticle formation; aggregation present
ZnO UV-Vis peak (post-pH adj.)	~360–380 nm (broadened)	Optimized colloidal stability; structural integrity maintained
Sunscreen UV peak 1	~250–270 nm	Phytochemical UV absorption (EGCG, glabridin)
Sunscreen UV peak 2	300–400 nm (broad)	ZnO-mediated broad-spectrum UV attenuation
Peak Absorbance (F2)	1.300 at 322 nm	Enhanced UVB/UVA border protection
Estimated SPF – F1	~2.84	Limited by sparse wavelength data points
Estimated SPF – F2	~12.34	430% improvement over F1 due to stable ZnO dispersion
pH (both formulations)	5.5	Skin-compatible; preserves stratum corneum integrity
Texture	Hydrogel (F2)	Cosmetically acceptable; lightweight and non-greasy
Colloidal Stability	High (pH 8.2 ZnO)	Prevents ZnO sedimentation; ensures consistent SPF delivery

5. CONCLUSION

This investigation successfully demonstrates the green synthesis of ZnO nanoparticles using an aqueous extract of Rubia cordifolia as a bioreductant and capping agent, with UV-Vis spectrophotometric confirmation of nanoparticle formation between 360 and 380 nm. The influence of pH on colloidal stability was clearly established: Batch 2 nanoparticles (pH 8.2) exhibited superior dispersibility and UV-blocking capacity relative to Batch 1 (pH 5.0). Herbal sunscreen formulations incorporating these biogenic ZnO nanoparticles in combination with green tea and licorice extracts demonstrated physicochemically acceptable properties, including a skin-compatible pH of 5.5, satisfactory spreadability, uniform texture, and water resistance in both formulations. The photoprotective superiority of Formulation 2, evidenced by an SPF of approximately 12.34 compared to 2.84 for Formulation 1, underscores the critical role of nanoparticle colloidal stability in determining final photoprotective efficacy. The additive UV-absorbing contributions of EGCG and glabridin complement the broad-spectrum UV attenuation provided by ZnO, supporting a multi-mechanism photoprotective strategy. Future investigations should incorporate advanced characterization techniques (XRD, FTIR, TEM, dynamic light scattering, and zeta potential analysis) to comprehensively characterize nanoparticle physicochemistry, alongside full-range SPF determination (290–400 nm) and in vivo clinical evaluation to establish translational utility.

6. LIMITATIONS

The current study was constrained by the non-availability of advanced characterization instrumentation, including X-ray diffraction (XRD), Fourier-transform infrared spectroscopy (FTIR), transmission electron microscopy (TEM), and zeta potential measurement facilities. These analyses would provide comprehensive information regarding nanoparticle crystallinity, surface functional groups, morphology, and long-term colloidal stability, respectively. Additionally, SPF estimation was conducted at a limited number of discrete wavelengths, which may underestimate true photoprotective capacity; full-spectrum analysis between 290 and 400 nm is recommended in subsequent investigations. Human participant clinical evaluation studies would further substantiate the translational relevance of the developed formulations.

ACKNOWLEDGEMENTS

The authors gratefully acknowledge Chhatrapati Shivaji Maharaj University, Panvel, Maharashtra, for providing laboratory infrastructure and research support. Special recognition is extended to MS. Shivani Pawar for her mentorship and technical guidance throughout the course of this investigation.

CONFLICT OF INTEREST

The authors declare no conflict of interest with respect to the authorship and publication of this article.

REFERENCES

1. Ichihashi M, Ueda M, Budiyanto A, et al. UV radiation-induced skin damage and molecular mechanisms of photocarcinogenesis. Photochem Photobiol Sci. 2005; 4(9):717–728.

2. Matsumura Y, Ananthaswamy HN. Toxic effects of UV radiation on the skin. Toxicol Appl Pharmacol. 2004; 195(3):298–308.

3. Smijs TG, Pavel S. Titanium dioxide and zinc oxide nanoparticles in sunscreens: focus on their safety and effectiveness. Nanotechnol Sci Appl. 2011; 4:95–112.

4. Haruna CA, Malik WA, Rijal MYS, Watoni AH, Ramadhan LOAN. Green Synthesis of Copper Nanoparticles Using Red Dragon Fruit (Hylocereus polyrhizus) Extract and Its Antibacterial Activity for Liquid Disinfectant. J Kim Sains Apl 2023;25(10):352-361.

5. Iravani S. Green synthesis of metal nanoparticles using plants. Green Chem. 2011; 13(10):2638–2650.

6. Patil SA, Bhagwat DA. Rubia cordifolia L.: a comprehensive review on phytochemistry, pharmacology, and therapeutic applications. J Ethnopharmacol. 2022; 280:114391.

7. Suzuki K, Koike H, Matsui H, et al. Beneficial effects of green tea catechins on photoprotection and skin health: a review. J Clin Biochem Nutr. 2010; 46(2):63–74.

8. Yokota T, Nishio H, Kubota Y, Mizoguchi M. The inhibitory effect of glabridin from licorice extracts on melanogenesis and inflammation. Pigment Cell Res. 1998; 11(6):355–361.

9. Chemat F, Rombaut N, Sicaire AG, et al. Ultrasound assisted extraction of food and natural products: mechanisms, techniques, combinations, and industrial applications. Ultrason Sonochem. 2017; 34:540–560.

10. Vijayakumar S, Mahadevan S, Arulmozhi P, et al. Green synthesis of zinc oxide nanoparticles using Atalantia monophylla leaf extract: characterization and pharmacological investigation. Biocatal Agric Biotechnol. 2018; 14:543–548.

11. Sonia S, Linda Jeeva Kumari H, Ruckmani K, Sivakumar M. Antimicrobial and antioxidant potentials of biosynthesized colloidal zinc oxide nanoparticles for a fortified cold cream formulation. Mater Sci Eng C. 2017; 79:581–589.

12. Alarifi S, Ali H, Alkahtani S, Alessia MS. Regulation of apoptosis through bcl-2/bax proteins expression and DNA damage by nano-sized zinc oxide. Int J Nanomed. 2017; 12:1939–1946.

13. Krishnaswamy K, Orsat V, Thangavel K. Synthesis and characterization of nano-encapsulated catechin by molecular inclusion with beta-cyclodextrin. J Food Eng. 2012; 111(2):255–264.

14. Dhingra D, Michael M, Rajput H, Patil RT. Dietary fibre in food: a review. J Food Sci Technol. 2012; 49(3):255–266.

15. Asl MN, Hosseinzadeh H. Review of pharmacological effects of Glycyrrhiza sp. and its bioactive compounds. Phytother Res. 2008; 22(6):709–724.

16. Guan LL, Lim HW, Mohammad TF. Sunscreens and photoaging: a review of current literature. Am J Clin Dermatol. 2021; 22(6):819–828.

17. Raj S, Jose S, Sumod US, Sabitha M. Nanotechnology in cosmetics: opportunities and challenges. J Pharm Bioallied Sci. 2012; 4(3):186–193.

18. Darlenski R, Sassning S, Tsankov N, Fluhr JW. Non-invasive in vivo methods for investigation of the skin barrier physical properties. Eur J Pharm Biopharm. 2009; 72(2):295–303.

19. Bala N, Saha S, Chakraborty M, et al. Green synthesis of zinc oxide nanoparticles using Hibiscus subdariffa leaf extract. RSC Adv. 2015; 5(7):4993–5003.

20. Monteiro-Riviere NA, Wiench K, Landsiedel R, et al. Safety evaluation of sunscreen formulations containing titanium dioxide and zinc oxide nanoparticles in UVB sunburned skin. Toxicol Sci. 2011; 123(1):264–280.

21. Sharma N, Jandaik S, Kumar S. Synergistic activity of doped zinc and copper oxide nanoparticles with antibiotics: ciprofloxacin, ampicillin, fluconazole and amphotericin B against pathogenic microorganisms. J Exp Nanosci. 2016; 11(13):1037–1050.

22. Ali A, Phull AR, Zia M. Elemental zinc to zinc nanoparticles: is ZnO NPs crucial for life? Synthesis, toxicological, and environmental concerns. Nanotechnol Rev. 2018; 7(5):413–441.